PHYSICAL REVIEW B **93**, 115146 (2016)

Bosonic topological phase in a paired superfluid

Snir Gazit and Ashvin Vishwanath
Department of Physics, University of California, Berkeley, California 94720, USA
(Received 29 October 2015; revised manuscript received 8 March 2016; published 30 March 2016)

We study an effective model of two interacting species of bosons in two dimensions, which is amenable to sign problem free Monte Carlo simulations. In addition to conventional ground states, we access a paired superfluid which is also a topological phase, protected by the remaining $U(1) \times \mathbb{Z}_2$ symmetry. This phase arises from the condensation of a composite object, the bound state of vortices and antivortices of one species, to a boson of the second species. We introduce a bulk response function, the Ising analog of the quantized Hall effect, to diagnose the topological phase. The interplay of broken symmetry and topology leads to interesting effects such as fractionally charged vortices in the paired superfluid. Possible extensions towards realistic models of cold atomic bosons are discussed.

DOI: 10.1103/PhysRevB.93.115146

I. INTRODUCTION

At low temperatures, interacting bosonic systems are expected to either be in a superfluid or an insulating phase. This classification follows from the conventional Landau theory which is based on symmetry breaking. Recently, it was realized that the insulating phase, in which the symmetry is preserved, can host additional phases characterized by nontrivial topological properties termed symmetry protected topological (SPT) phases [1].

More broadly, SPT phases are defined through an equivalence relation between ground states of gapped Hamiltonians that are symmetric under a symmetry group G and have no topological order (i.e., a unique ground state on a closed manifold). Two SPT phases are then said to be in the same equivalence class if they can be adiabatically connected without breaking the symmetry. These considerations have led to a classification based on the Borel-group-cohomology [2], cobordism [3], K-matrix theory [4], and nonlinear sigma models [5].

In the bosonic case, SPT phases are stable only in the presence of strong correlations since in the weakly interacting limit bosons inevitably condense. This is in sharp contrast to the noninteracting, band structure picture of electronic topological insulators.

Experimentally, the topologically protected spin one half edge states of the Haldane chain, a prime example of SPT phases in one spatial dimension [6], have been observed in neutron scattering experiments on Y_2BaNiO_5 compounds [7]. However, in spatial dimensions greater than one, bosonic SPT phases have not been demonstrated experimentally yet. In that regard, cold atomic systems, with their high flexibility in manipulating lattice structures and interactions [8], offer a promising experimental testbed for future realizations of SPT phases.

In certain cases, the physical mechanism underlying the SPT phase is based on real space binding of symmetry charges to topological defects [9,10]. A notable example is the bosonic quantum Hall (BQH) state [4,11] that can be realized by binding particles (holes) to vortex (antivortex) defects [12]. Proliferating the charge decorated vortices gives rise to a topologically nontrivial insulating state characterized by a Hall conductance that is quantized to even integers $\sigma_{xy} = 2\,n\,e^2/h$. In a similar manner, binding vortices to spin degrees of freedom yields a time reversal invariant SPT phase [13].

Despite the appeal of the above mentioned approaches, current proposals pose experimental difficulties. More specifically, the BQH state breaks time reversal symmetry (TRS) and models realizing it [14–18] require a strong magnetic field or significant magnetic flux [19] within a unit cell. In this extreme regime, the BQH state competes with fractional and even non-Abelian topological phases. One may have hoped that realizing the BQH, a bosonic analog of the integer quantum Hall state, would be less demanding.

In this paper, we construct a two dimensional bosonic SPT phase that respects TRS and is composed solely of bosonic degrees of freedom. We implement our program of creating and identifying properties of this phase in an effective loop model using a sign problem free Monte Carlo (MC) simulation. To identify the SPT phase we introduce a procedure that directly measures the topological response of the SPT phase. In addition, we study the protected gapless edge states on a cylindrical geometry.

II. PROPOSED CONSTRUCTION

The construction is briefly summarized as follows. We begin with two species of bosons, labeled by A and B, with $U(1) \times U(1)$ symmetry corresponding to particle number conservation of each species separately. Let us assume that both species are in a superfluid phase. We then bind *both* the vortices and the antivortices of type A to the bosons of B, and condense this composite object. The choice of binding to bosons (rather than vacancies as in the BQH state) is crucial to ensure time reversal symmetry.

Condensing the charged A vortices forms an insulator, while B bosons remain in a superfluid state. However, the superfluid is one of boson pairs, so the original symmetry is broken down to $U(1) \times \mathbb{Z}_2$. This residual symmetry protects a bosonic topological phase with nontrivial edge states.

To see why this particular composite object condensate corresponds to a pair condensate, let us label the two composite objects that we are condensing as $\psi_+ = v_A b_B$ and $\psi_- = v_A^\dagger b_B$, where $v_A^\dagger$ (v_A) is the vortex creation (annihilation) operator and b_B is the bosonic annihilation operator. Note,

a condensate implies $\langle\psi_+\rangle, \langle\psi_-\rangle \neq 0$. However, from this we cannot conclude that the B boson is condensed since vortices are nonlocal objects. The vorticity free combination that is condensed though is $\langle\psi_+\psi_-\rangle = \langle b_B b_B\rangle \neq 0$, giving rise to a pair condensate.

It is worth noting two points at this stage. First, the symmetric charge assignment may be argued to be easier to realize. The vortex core is associated with a reduced boson density. Assuming a repulsive interaction between the two species of bosons, the vortex (and equally the antivortex) will be seen as a potential well for the opposite species of boson, potentially leading to a bound state. We caution that obtaining this binding is one of several ingredients required to create the desired phase. Second, we note that the symmetry group protecting the SPT phase is a residual symmetry obtained by spontaneous symmetry breaking. This situation, to the best of our knowledge, has not been discussed before in the context of bosonic SPT phases. It provides a physical mechanism for introducing "gauge defects" that were suggested previously as theoretical devices to probe bosonic SPT phases [20]. Here for example, the pair condensate admits π (or half) vortex defects, which are predicted to carry a half charge of the unbroken $U(1)$ symmetry of type A bosons.

Similar to the trivial Bose insulator, condensing the $\mathbb{Z}_2$ charged vortices results in a $U(1)$ symmetric state [21–23]. In addition, the $\mathbb{Z}_2$ symmetry is restored. This can be argued by noting that since the vortex is a nonlocal object one cannot define a local order parameter for the bounded $\mathbb{Z}_2$ charges and thus the symmetry is preserved.

The above can also be understood by a simple geometrical argument based on a world-line picture. Following the usual quantum to classical mapping [24], the partition function of a $\mathbb{Z}_2$ symmetric quantum system in d spatial dimensions can be reformulated as a statistical mechanics model of unoriented loops [as opposed to $U(1)$ symmetry for which the loops are oriented] defined on a $d+1$ dimensional Euclidean space-time. In this language, the world lines carry a $\mathbb{Z}_2$ charge and the total $\mathbb{Z}_2$ charge, $\mathcal{C}_{\mathbb{Z}_2}$, equals the parity of world-line crossings at any given imaginary time slice.

Let us recall the description of the conventional phases in this picture. In the disordered phase, the loop fugacity is small and hence a typical loop configuration consists out of small closed loops. In particular, winding around the imaginary time axis is suppressed by the finite single particle gap. As a result, the number of world lines crossing, at any given imaginary time slice, is even and hence $\mathcal{C}_{\mathbb{Z}_2} = 0$, as expected. By contrast, the ordered phase, where the loop fugacity is large, is characterized by large loops that can wind around the imaginary time axis giving rise to fluctuations in $\mathcal{C}_{\mathbb{Z}_2}$ and breaking of the $\mathbb{Z}_2$ symmetry.

Turning back to the nontrivial SPT phase, here the $\mathbb{Z}_2$ world lines are bounded to the world lines of the condensed vortices as depicted in Fig. 1(a). Seemingly, the large $\mathbb{Z}_2$ loops could potentially lead to fluctuations of $\mathcal{C}_{\mathbb{Z}_2}$ and breaking of the $\mathbb{Z}_2$ symmetry. To understand why this is not the case, we note that on a closed manifold the total vorticity charge is neutral [25]. This topological constraint restricts the number of vortex world lines threading any imaginary time plane to be even. Consequently, also the total $\mathbb{Z}_2$ charge is even, i.e., $\mathcal{C}_{\mathbb{Z}_2} = 0$, yielding a disordered state.

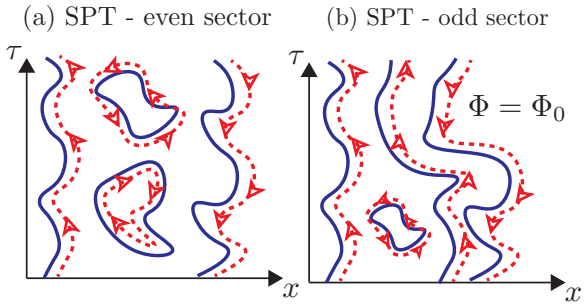

FIG. 1. Typical world-line configurations in the SPT phase. Blue lines and red lines correspond to the $\mathbb{Z}_2$ world lines and the vorticity current, respectively. Threading a unit of flux quantum shifts the total $\mathbb{Z}_2$ charge from the (a) even to the (b) odd sector.

III. SPT INVARIANTS

The symmetry is preserved both in the trivial and nontrivial SPT phases and hence they cannot be distinguished based on symmetry probes. The topological invariants characterizing different SPT phases are uncovered by gauging [20,26,27] the symmetry and examining the emergent topological field theory.

To see how this applies in our case, it is useful to first consider the minimal BHQ state with $\sigma_{XY} = 2$, which at low energies can be described by an effective two component, $a_{I=A/B}$, mutual Chern-Simons (CS) theory [4],

$$\mathcal{L} = \frac{1}{4\pi}(\epsilon^{\mu\lambda\nu} a_{A,\mu}\partial_\lambda a_{B,\nu} + A \leftrightarrow B). \tag{1}$$

Coupling the $U(1)$ currents, $J^\mu_I = \epsilon^{\mu\lambda\nu}\partial_\lambda a_{I,\nu}$, to an external probe gauge field $\mathcal{A}_{A/B,\nu}$ yields a quantized mutual Hall response, $J^\mu_{A/B} = \frac{1}{2\pi}\epsilon^{\mu\lambda\nu}\partial_\lambda \mathcal{A}_{B/A,\nu}$. Returning to our case, we now introduce a Higgs term [26] which breaks the $U(1)$ symmetry of type B boson down to $\mathbb{Z}_2$, such that its charge is now identified only modulo two. The resulting topological response is then an Ising version of the quantum Hall effect, since threading an external unit of flux quantum, $\Phi_0 = 2\pi$, of the $U(1)$ symmetry generates a $\mathbb{Z}_2$ charge.

In terms of the world-line picture, see Fig. 1(b), threading a unit of flux quantum induces one additional unit of vorticity that, in the SPT phase, carries a $\mathbb{Z}_2$ charge. As a result, the total $\mathbb{Z}_2$ charge shifts from the even to the odd sector, namely $\mathcal{C}_{\mathbb{Z}_2} = 1$. Repeating the same analysis in the topologically trivial phase would have no effect since the $\mathbb{Z}_2$ charges are decoupled from the vortices.

An interesting consequence of the enlarged $U(1)\times U(1)$ symmetry is that the pair condensed state supports half-vortex excitation of type B bosons carrying one-half flux quantum $\Phi^B_{1/2} = \pi$ [28]. Following the mutual Hall response in Eq. (1), $j^0_A = \Phi^B_{1/2}/2\pi = 1/2$, we see that a fractional one-half $U(1)$ charge of type B rotors is bounded to the π-vortex core.

IV. COUPLED ROTOR MODEL AND OBSERVABLES

To demonstrate numerically the above phenomenological approach, we study a classical statistical mechanics model defined on a discrete 2+1 dimensional Euclidean space-time lattice. The degrees of freedom are two species of planar rotors

parametrized by θ_A and θ_B that reside on the vertices, r_i and R_i, of the direct and dual cubic lattice, respectively. The partition function is given by

$$\mathcal{Z}[\alpha_A,\alpha_B,\lambda] = \int \mathcal{D}\theta_A \mathcal{D}\theta_B f_{\alpha_A}(\theta_A) f_{\alpha_B}(\theta_B) g_\lambda(\theta_A,\theta_B). \quad (2)$$

Here, $f_\alpha(\theta) = \prod_{i,\mu} V_\alpha(\theta_i - \theta_{i+\hat{\mu}})$, with $\mu = x,y,\tau$, is a generalized XY model with nearest neighbor Boltzmann weight $V_\alpha(x) = 1 + 2e^{-\alpha}\cos(x)$. The above three dimensional XY model captures the low energy properties of two dimensional lattice bosons with particle-hole symmetry (integer filling) [29]. The atypical choice for the Boltzmann weight is designed such that in the dual loop current representation [30] the integer bond currents $J_{i,\mu}$ are restricted to the values $J_{i,\mu} = 0, \pm 1$. In the quantum analogy, we allow only a single particle or hole excitation at each site.

The coupling between the rotor models, $g_\lambda(\theta_A,\theta_B) = e^{-\lambda \mathcal{S}_C[\theta_A,\theta_B]}$, is tuned by the coupling constant λ and is defined through the binding action,

$$\mathcal{S}_C = \sum_i \left[\left(|J^B_{R_i,\mu}| - |Q^A_{R_i,\mu}|\right)^2\right]. \quad (3)$$

Here, $J^B_{R_i,\mu}$ is the integer bond current of type B bosons, defined before, and $Q^A_{R_i,\mu}$ is the vorticity three-current of type A rotors. In defining the vorticity current we will consider the more general case where we thread a finite magnetic flux density $\phi = \Phi/L^2$, with L being the linear system size. To do so, we minimally couple the bond current of type A rotors to an external gauge field $\mathcal{A}_{r_i,\mu}$ through a Peierls substitution, $\mathcal{J}^A_{r_i,\mu} = (\theta^A_{r_i} - \theta^A_{r_i+\hat{\mu}}) \bmod 2\pi \to (\theta^A_{r_i} - \theta^A_{r_i+\hat{\mu}} - \mathcal{A}_{r_i,\mu}) \bmod 2\pi$. The vorticity current is then given by the lattice curl, $2\pi Q^A_{R_i,\mu} + \phi_{R_i,\mu} = \nabla \times \mathcal{J}^A$. The magnetic flux density $\phi_{R_i,\mu} = \phi\delta_{\mu,\tau}$ is uniform and it is nonvanishing only along the imaginary time direction. The vorticity is quantized to integers and on a cubic lattice it is restricted to the values $Q^A_{R_i,\mu} = 0, \pm 1$.

Possible symmetry breaking is probed through the condensate fraction,

$$C_{1/2} = \frac{1}{L^3}\sum_r g_{1/2}(r), \quad (4)$$

where $g_1(r) = \langle e^{i(\theta_i - \theta_{i+r})}\rangle$ and $g_2(r) = \langle e^{i2(\theta_i - \theta_{i+r})}\rangle$ are the single particle and pair correlation functions, respectively. Pair condensation can also be detected from the winding number distribution, $P(W_\tau)$. The winding number, $W_\tau = 1/L_\tau \sum_i J_{i,\tau}$, equals the total current along the imaginary time direction and can be interpreted as the total $U(1)$ charge in the quantum language. In a pair condensate, the probability for odd winding numbers vanishes, $P(W_\tau | W_\tau \text{ is odd}) = 0$ [31].

A key ingredient of our analysis is identifying an order parameter that discriminates the nontrivial SPT phase from the trivial disordered phase. In our model the symmetry ($\mathbb{Z}_2$) and its corresponding gauge field are discrete and hence linear response based observables, such as the quantized Hall conductance in the BQH case, cannot be defined. To resolve this, we follow the world-line picture by measuring $\mathcal{C}_{\mathbb{Z}_2}$ in the presence of a single flux quantum. A shift in $\mathcal{C}_{\mathbb{Z}_2}$ from the even to the odd sector serves as an order parameter that captures the topological response of this phase. In terms of the physical $U(1)$ degrees of freedom of type B rotors, $\mathcal{C}_{\mathbb{Z}_2}$ is defined through the winding number parity

$$\mathcal{C}_{\mathbb{Z}_2} = \left\langle \frac{1}{2}(1 - (-1)^{W_\tau}) \right\rangle. \quad (5)$$

V. METHODS

We evaluate the partition function in Eq. (2) by means of a classical Monte Carlo. Type A (B) rotors are represented in the phase (bond current) representation. This choice enables us to evaluate the binding action in Eq. (3) since both the vortex current, Q^A, and the bond current, J_B, can be readily computed in this representation. The closed loop configurations of type B rotors are sampled using the classical worm algorithm (WA) [32]. In most cases we set the system size to be $L = 16$, a value for which finite size corrections are controlled. To check the convergence of our results with system size and to perform finite size scaling analysis we considered system sizes up to $L = 32$. Further details on the MC algorithm can be found in Appendix B.

VI. RESULTS

In this section, we construct the phase diagram (Fig. 2) of the coupled rotor model in Eq. (2). Within the range of parameters investigated we found three phases. Two of them, denoted by phase I and phase II, can be classified according to different patterns of $U(1)$ symmetry breaking. In addition, we find a nontrivial SPT phase, that is distinct from the trivial disordered state.

The classification to phases is performed in two steps. First we classify the phases according to $U(1)$ symmetry breaking of A and B rotors. Following that we identify the SPT phase by numerically measuring the SPT invariant and studying the protected gapless edge states in a cylindrical geometry.

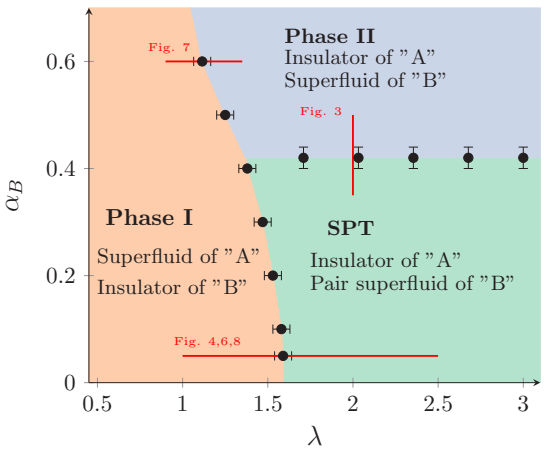

FIG. 2. Phase diagram of the coupled rotor model in Eq. (2) as a function of α_B and λ for $\alpha_A = 4$. The numerically computed critical points are marked by black circles. We probed $U(1)$ symmetry breaking by using the condensate fraction. The SPT phase, which is also a paired superfluid of type B rotors, is identified by measuring the topological response to an external flux. Red lines correspond to parameter cuts along which we perform finite size scaling scans in the labeled figures.

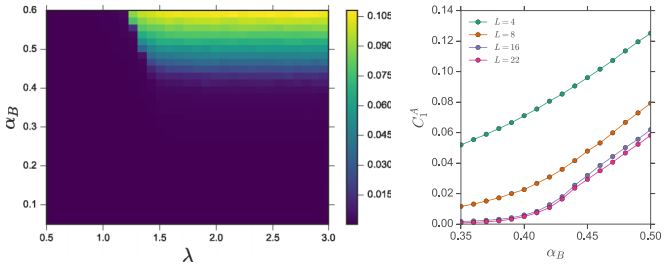

FIG. 3. Single particle condensate fraction of type A rotors. (a) The condensate fraction, C_1^A, is nonvanishing only in phase II, where λ and α_B are sufficiently large. (b) Ordering transition of type A rotors for $\lambda = 2$ as a function of α_B and for system sizes $L = 4,8,16,22$.

A. $U(1)$ symmetry breaking

In the decoupled limit, i.e., $\lambda = 0$, both rotors undergo an ordering transition belonging to the three dimensional XY model universality class. We locate the critical point between the ordered and disordered phase using the standard finite size scaling analysis of the superfluid stiffness [29,33]. We find that the critical coupling equals $\alpha_c = 1.50(1)$.

According to the phenomenological description of Sec. II, the SPT phase is realized by condensing a bound state of type A vortex and type B charge. This is possible only if both components, type A vortex *and* type B charge, are not gapped. To achieve that, in the following, we set $\alpha_A = 4 > \alpha_c$ and focus on the parameter range $\alpha_B < \alpha_c$. This choice of parameters ensures that, in the decoupled limit, type A (B) rotors are in the disordered (ordered) phase.

We map the phase diagram as a function of λ and α_B on an evenly spaced grid of 32 points for the range of values $\lambda \in [0.5,3]$ and $\alpha_B \in [0.05,0.6]$.

In Fig. 3(a) we depict the single particle condensate fraction, C_1^A, of type A rotors. In most parts of the phase diagram the condensate fraction vanishes indicating on a disordered phase, which is expected from the choice $\alpha_A > \alpha_c$.

Interestingly, for sufficiently large α_B and λ the condensate fraction, C_1^A, is finite, implying on an ordered superfluid phase. To understand this result, we note that for large λ, type A vortices can form only in the presence of type B charges, and these charges are suppressed when increasing α_B. The combined effect gaps type A vortices altogether and gives rise to a condensate of type A rotors.

In Fig. 3(b) we study the convergence of our results with size near the transition. We set $\lambda = 2.0$ and cross the phase transition towards phase II by increasing α_B. The condensate fraction is well converged within the largest system size considered, $L = 22$.

The single particle condensate fraction, C_1^B, of type B rotors is shown in Fig. 4(a). For weak binding, λ, type B rotors are condensed as evident from the finite condensate fraction. As before, in the decoupled limit this result is expected since we consider the parameter range $\alpha_B < \alpha_c$. Increasing the binding strength, λ, leads to a phase transition at a critical binding strength $\lambda_c(\alpha_B)$ that is marked by the vanishing of C_1^B.

The above result does not necessarily imply that the $U(1)$ symmetry of type B rotors is completely restored. Motivated

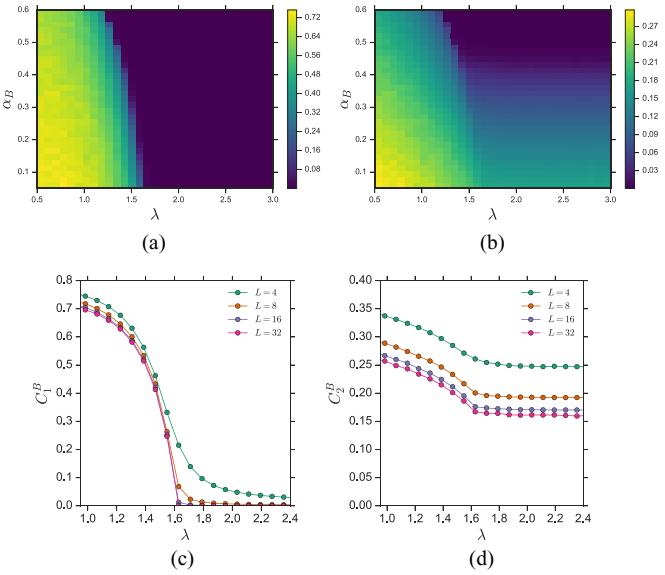

FIG. 4. Single and pair condensate fraction of type B rotors. (a) For small values of λ the condense fraction is finite and it vanishes at a critical coupling $\lambda_c(\alpha_B)$. (b) The pair condensate function, C_2^B, remains finite even for $\lambda > \lambda_c(\alpha_B)$ and sufficiently small α_B. (c),(d) Finite size scaling analysis of the phases' transition for $\alpha_B = 0.05$ as a function of λ and for system sizes $L = 4,8,16,32$.

by the phenomenological construction of the SPT phase, we expect that an increase in λ would result in an instability towards a SPT phase, in which the charged vortex condensate forms a paired superfluid of type B rotors.

To test this scenario, in Fig. 4(b), we study the pair condensate fraction, C_2^B. We see that for sufficiently small values of α_B, the pair condensate fraction remains finite even for $\lambda > \lambda_c(\alpha_B)$, where C_1^B vanishes. This result indicates on the emergence of a paired superfluid of type B rotors. In contrast, in phase II, both C_1^B and C_2^B vanish such that type B rotors are disordered. This behavior can be understood following the same reasoning presented before for the condensation of type A rotors in phase II.

In Figs. 4(c) and 4(d) we perform a finite size scaling analysis of the transition to test the convergence of the numerical result with system size. Specifically, we take $\alpha_B = 0.05$ and cross the transition by increasing λ. We find that for the largest system we considered, $L = 32$, the results are well converged in both phases and display small deviation with system size.

We further verify the formation of a pair superfluid by studying the winding number distribution for $\alpha_B = 0.05$ in Fig. 5. For $\lambda = 1.22 < \lambda_c$, type B rotors are condensed as evident from the broad distribution of $P(W_\tau)$. For $\lambda = 2.83 > \lambda_c$, while the distribution remains broad, the probability for odd winding numbers vanishes. This serves as additional evidence for the formation of a pair condensate.

The winding number distribution analysis can also be interpreted in the context of the $2+1$ dimensional quantum picture of the SPT phase. In this language the winding number is identified with the deviation of the bosonic particle number, δn_B, from integer filling. The emergent $\mathbb{Z}_2$ symmetry then corresponds to the parity of δn_B.

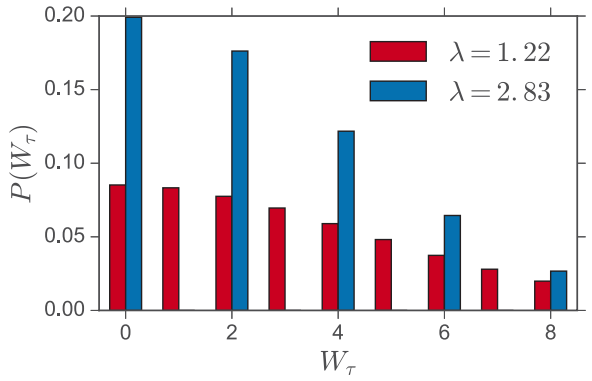

FIG. 5. Winding number distribution, $P(W_\tau)$, for $\alpha_B = 0.05$. Below the critical coupling (red), $\lambda = 1.22 < \lambda_c$, we find a broad distribution corresponding to a superfluid. Above the critical coupling (blue), $\lambda = 2.83 > \lambda_c$, the distribution remains wide but the probability for odd number of particles vanishes, $P(W_\tau | W_\tau \text{ is odd}) = 0$, indicating on a paired superfluid.

It is interesting to investigate the nature of the different phase transitions appearing in Fig. 2. We first consider the phase transition between phase I and the pair superfluid. The transition is marked by spontaneous symmetry breaking of a $\mathbb{Z}_2$ symmetry and if, in addition, it is continuous we expect it to belong to the three dimensional Ising universality class.

To check this prediction we study the critical properties of the total $\mathbb{Z}_2$ charge, $\mathcal{C}_{\mathbb{Z}_2}$. In phase I the symmetry is broken and hence $\mathbb{Z}_2$ fluctuates and averages to one-half, whereas in the paired superfluid phase the $\mathbb{Z}_2$ symmetry is restored and therefore $\mathcal{C}_{\mathbb{Z}_2} = 0$. Since $\mathcal{C}_{\mathbb{Z}_2}$ is a dimensionless quantity we expect it to attain a universal value at criticality.

We can therefore consider the following scaling form for $\mathcal{C}_{\mathbb{Z}_2}$ near the critical point,

$$\mathcal{C}_{\mathbb{Z}_2}(\delta\lambda, L) = g(\delta\lambda L^{1/\nu}). \tag{6}$$

Here $\delta\lambda = \frac{\lambda - \lambda_c}{\lambda_c}$, $g(x)$ is a universal scaling function, and ν is the correlation length critical exponent.

In Fig. 6(a) we depict $\mathcal{C}_{\mathbb{Z}_2}$ for $\alpha_B = 0.05$ near the critical coupling for system sizes $L = 8, 16, 32$. Curves for different system size cross at a single point. By locating the crossing point, we determine the critical coupling $\lambda_c = 1.597(1)$ and the universal value at the crossing $g(0) = 0.230(5)$. We employed this method to locate the phase transitions between phase I and the pair superfluid, in Fig. 2.

In Fig. 6(b) we perform a finite size scaling curve collapse. We center the horizontal axis around the critical coupling and scale it according to Eq. (6), i.e., $\delta g \to \delta g L^{1/\nu}$. For the correlation length critical exponent we take $\nu = 0.6296(3)$, its value at the three dimensional Ising model universality class as was computed by high precision classical MC simulation [34]. Indeed, we find that curves for different system sizes collapse into a single universal curve with high precision. A more detailed investigation of the critical properties, in particular an independent estimation of the critical exponents would entail the use of larger system sizes which are beyond the reach of our numerics.

Next, we consider the phase transition between phase I and phase II. Here, the two phases are characterized by

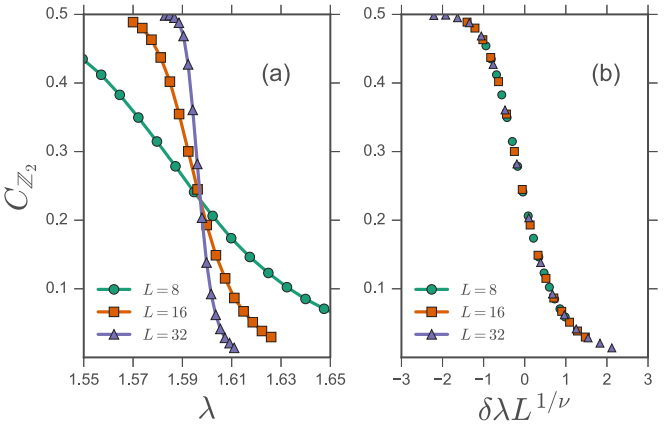

FIG. 6. Finite size scaling analysis of total $\mathbb{Z}_2$ charge, $\mathcal{C}_{\mathbb{Z}_2}$, at the phase transition between phase I and the paired superfluid, for $\alpha_B = 0.05$. $\mathcal{C}_{\mathbb{Z}_2}$ is a dimensionless observable and thus it is expected to obtain a universal value at the critical point. This behavior is clearly since in panel (a) where curves for different system size cross at the critical coupling, $\lambda_c = 1.597(1)$, with small dependence on system size. (b) Finite sizes scaling curve collapse. The horizonal axis is rescaled according to Eq. (6).

spontaneous symmetry breaking of two *different* symmetries [$U(1)$ symmetry of type A and B rotors]. As a consensus, based on Landau theory, without further fine-tuning of the parameters the transition is expected to be generically first order.

To test this numerically, we investigate the absolute value of type B bond current $\langle |J_B| \rangle$. This observable serves as a measure for the classical energy of type B rotors [32]. At a first order phase transition the distribution of $\langle |J_B| \rangle$ is expected to develop a double peak structure corresponding to the coexistence of the two phases.

In Fig. 7 we fix $\alpha_B = 0.6$ and depict histograms of $\langle |J_A| \rangle$ at the critical coupling and slightly below and above. At $\lambda = 1.16 \approx \lambda_c$ the histogram displays a double-peak structure, whereas below and above the transition only a single peak is

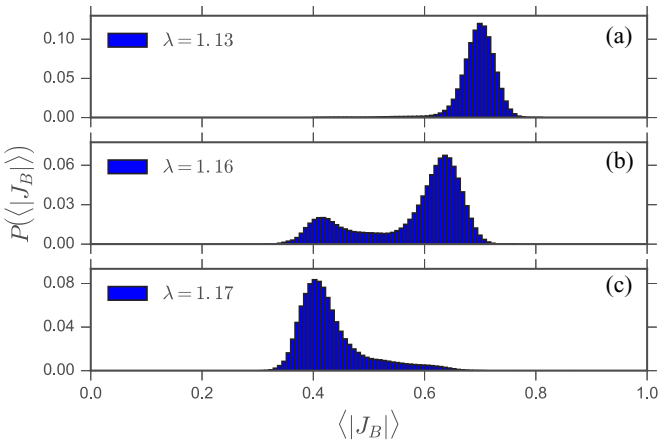

FIG. 7. Probability histogram of $\langle |J_A| \rangle$ for $\alpha_B = 0.6$. (b) At the critical binding, $\lambda_c = 1.16$, the histogram develops a double peak structure corresponding to coexistence of phase I and phase II and indicating on a first order phase transition. (a),(c) By contrast, slightly above and below the critical point the histograms consist of a single peak.

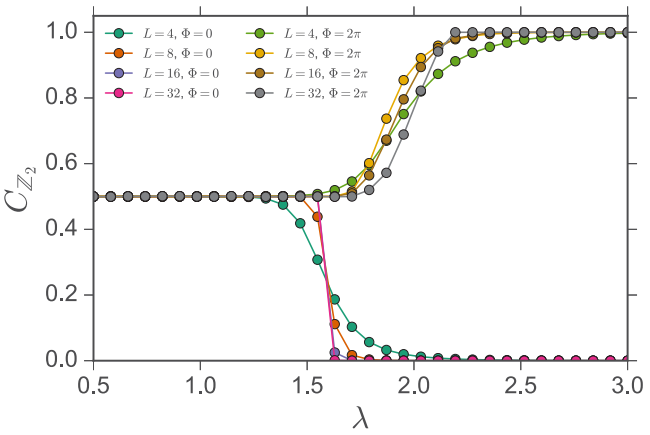

FIG. 8. Total $\mathbb{Z}_2$ charge of type B rotors as a function λ for $L = 4,8,16,32$, $\alpha_B = 0.05$ and for magnetic flux $\Phi_A = 0$ and $\Phi_A = 2\pi$. In phase I, $\lambda < \lambda$, $\mathcal{C}_{\mathbb{Z}_2}$ fluctuates and average to $1/2$. For $\lambda > \lambda_c$, in the absence of an external magnetic flux $\mathcal{C}_{\mathbb{Z}_2}$ vanishes as expected in a paired superfluid. Threading a magnetic flux $\Phi_A = 2\pi$ shifts the $\mathcal{C}_{\mathbb{Z}_2}$ charge from the even to the odd sector of the theory, i.e., $\mathcal{C}_{\mathbb{Z}_2} = 1$.

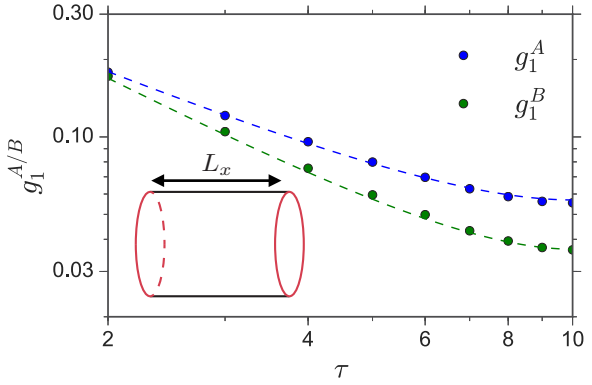

FIG. 9. Single particle Green's function, $g_1^{A/B}$, evaluated along the edges of a cylindrical. The simulation parameters are $L_y = L_\tau = 20$, $L_x = 8$, $\alpha_B = 0.05$, and $\lambda = 2.5$. Solid lines are a numerical fit to the power law form in Eq. (7).

seen. This analysis validates our expectation for a first order phase transition.

In a similar manner, the transition between phase II and the paired superfluid involves a simultaneous breaking of two distinct symmetries and hence it is expected to be first order. We were unable to confirm this prediction in our numerics due to the relatively small systems sizes that are accessible to our Monte Carlo simulation.

Summarizing the above results, we conclude that the pair condensed phase has an unbroken $U(1) \times \mathbb{Z}_2$ symmetry and hence it is a candidate for a nontrivial SPT phase.

B. SPT invariant and gapless edge states

Our main result is presented in Fig. 8, where we depict $\mathcal{C}_{\mathbb{Z}_2}$ as a function of λ both for $\Phi = 0$ and $\Phi = \Phi_0$. For $\lambda < \lambda_c$, type B rotors are condensed and thus the charge parity, $\mathcal{C}_{\mathbb{Z}_2}$, fluctuates and averages to one-half. At $\lambda = \lambda_c$, $\mathcal{C}_{\mathbb{Z}_2}$ jumps abruptly to zero as the $\mathbb{Z}_2$ symmetry corresponding to the charge parity is restored. We now thread the torus with a single flux quantum; the charge parity rises to $\mathcal{C}_{\mathbb{Z}_2} = 1$, where the pair condensate forms. This provides a direct measurement of the topological response of the SPT phase.

Finally, we study the edge states in the SPT phase on a cylindrical geometry. Gapless excitations are expected to follow an asymptotic power-law form proportional to

$$g_1^{A/B}(\tau) \sim (\tau^{-\gamma_{A/B}} + (\beta - \tau)^{-\gamma_{A/B}}). \tag{7}$$

We compute the single particle Green's function of both rotors along the edges of the cylinder for $\alpha_B = 0.05$ and $\lambda = 2.5$, as plotted in Fig. 9.

We numerically fit the MC data to the above form and find good agreement with the exponents $\gamma_A = 1.0(1)$ and $\gamma_B = 1.3(1)$. Importantly, we have also explicitly verified that the bulk remains gapped. In the SPT phase, the two edge modes are conjugate variables [4,12] and hence their Luttinger liquid parameters are related by a T-duality $\gamma_A \times \gamma_B = 1$, as shown in Appendix A. Numerically we find $\gamma_A \times \gamma_B \approx 1.3(2)$. The small deviation from the analytic prediction is most likely related to finite size effects.

VII. DISCUSSION AND SUMMARY

Realizing a SPT phase in cold atomic systems requires better understanding of physical mechanisms leading to binding of vortices to charge degrees of freedom, and condensation of these composite objects. While we have used a loop model for convenience, in the future we anticipate microscopic implementations utilizing a lattice Hamiltonian bosonic model. Translating terms from our loop model to the Hamiltonian formulation provides guidance along this direction. For example, one promising approach is to introduce correlated hopping terms that were recently suggested in lattice realization of the BQH state [16]. Alternatively, a modified version of the two-component bosnic model studied in [35] might sustain the SPT phase. We plan to apply this method to our model in a future study.

As a concrete experimental signature for the SPT phase, in cold atomic systems, we propose to probe the fractional one-half charges bounded to the π vortices. Rotating the optical lattice can, in principle, induce vortices [36], and the fractional charge can be measured by *in situ* imaging [37]. We do not directly demonstrate this effect in the numerical MC simulation since it introduces a sign problem.

More generally, our numerical method for measuring the topological response of certain SPT phases protected by *discrete* symmetry in MC simulations can be applied to other examples of SPT phases with different symmetries and dimensionality.

Summarizing, we proposed a purely bosonic model that following pair condensation realizes a SPT phase protected by $U(1) \times \mathbb{Z}_2$ symmetry. The signatures of the SPT phase were probed in an effective lattice model, and the interplay with spontaneous symmetry breaking was discussed. Our approach could guide the search for possible realizations of SPT phases in realistic models.

ACKNOWLEDGMENTS

We thank Itamar Kimchi, Ehud Altman, Mike Zaletel, Yuan Ming Lu, Norman Yao, and Ribhu Kaul for discussions, and

acknowledge support from the Templeton Foundation and AFOSR MURI Grant No. FA9550-14-1-0035. S.G. received support from the Simons Investigators Program and the California Institute of Quantum Emulation. This research was done using resources provided by the Open Science Grid [38,39], which is supported by the National Science Foundation and the U.S. Department of Energy's Office of Science.

APPENDIX A: SINGLE PARTICLE GREEN'S FUNCTION FOR GENERAL EDGE INTERACTIONS

The low energy description of the edge in the SPT phase is given by the action

$$\mathcal{L} = \frac{1}{4\pi}\int dx\,dt\Big(\partial_t\phi_1\partial_x\phi_2 + \partial_t\phi_2\partial_x\phi_1 + \sum_{I,J=1.2} V_{I,J}\partial_x\phi_I\partial_x\phi_J\Big). \tag{A1}$$

The matrix $V_{I,J}$ is nonuniversal and corresponds to interactions between the edge modes. The $K = \left(\begin{smallmatrix}0 & 1\\ 1 & 0\end{smallmatrix}\right)$ and V_{IJ} matrices can be diagonalized simultaneously since K is symmetric and V is symmetric and positive definite [40]. Explicitly, we define

$$\phi_1 = \frac{1}{\sqrt{2g}}(X_L + X_R),$$
$$\phi_2 = \sqrt{g/2}(X_R - X_L),$$

where $g = \sqrt{V_{11}/V_{22}}$. Substituting in Eq. (A1) gives

$$\mathcal{L} = \frac{1}{4\pi}\int dx\,dt[\partial_x X_R(\partial_t - v_R\partial_x)X_R + \partial_x X_L(-\partial_t - v_L\partial_x)X_L], \tag{A2}$$

where the right and left movers velocities are $V_{R/L} = \sqrt{V_{11}V_{22}} \pm V_{12}$,

The two point Green's function is then given by

$$\left\langle e^{i(\phi_1(x,t)-\phi_1(0,0))}\right\rangle \propto \prod_{R/L}|x - v_{R/L}t|^{g},$$
$$\left\langle e^{i(\phi_2(x,t)-\phi_2(0,0))}\right\rangle \propto \prod_{R/L}|x - v_{R/L}t|^{1/g}.$$

From the above equations we see that the product of the Luttinger liquid parameters is unity.

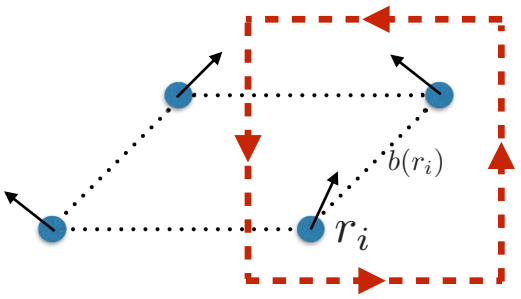

FIG. 10. Combined MC move. A planar angle $\theta_A(r_i)$ is drowned randomly and a bond current loop of type B rotors belonging to the dual lattice and surrounding the bond $b(r_i)$ is constructed.

APPENDIX B: MONTE CARLO ALGORITHM IMPLEMENTATION DETAILS

In this section we provide a more detailed description of the MC algorithm used to compute the classical partition function in Eq. (2). As mentioned in the main text, we reformulated the action of type B rotors as an integer bond current model. The closed loop configuration is sampled using the worm algorithm [32,41]. Type A rotors were represented by an angle variable and we employed the usual Metropolis-Hastings single site update scheme.

In the pair condensed phase, worm updates of a single field insertion, $e^{i\theta}$, are inefficient due to the finite single particle gap. To address this we introduced updates in which the worm's head carries two field insertions, $e^{i2\theta}$. This also enabled us to directly measure the pair correlation function [31].

In the SPT phase, where the coupling λ is sizable, MC moves that sample A and B rotors separately are inefficient since they must overcome an energy barrier in order to generate a bound state of a $\mathbb{Z}_2$ charge and a vortex.

To overcome this difficulty we introduced the following MC move, depicted schematically in Fig. 10. First, we propose an angle update to a type A rotor at a randomly selected site r_i (belonging to the direct lattice). Such a move can potentially generate a vortex loop. We then randomly select a direct lattice bond $b(r_i)$ out of the bonds emanating from the site r_i. Finally, we suggest constructing a loop current of type B rotors surrounding the bond $b(r_i)$ in the dual lattice. The move is accepted or rejected according to the *total* Boltzmann ratio. We found that this simple move allows the formation of $\mathbb{Z}_2$ charged vortex loops and the resulting MC correlation time was significantly reduced.

[1] X. Chen, Z.-C. Gu, Z.-X. Liu, and X.-G. Wen, Science **338**, 1604 (2012).
[2] X. Chen, Z.-C. Gu, Z.-X. Liu, and X.-G. Wen, Phys. Rev. B **87**, 155114 (2013).
[3] A. Kapustin, arXiv:1403.1467.
[4] Y.-M. Lu and A. Vishwanath, Phys. Rev. B **86**, 125119 (2012).
[5] Z. Bi, A. Rasmussen, K. Slagle, and C. Xu, Phys. Rev. B **91**, 134404 (2015).
[6] F. Pollmann, E. Berg, A. M. Turner, and M. Oshikawa, Phys. Rev. B **85**, 075125 (2012).
[7] J. Darriet and L. Regnault, Solid State Commun. **86**, 409 (1993).
[8] I. Bloch, J. Dalibard, and W. Zwerger, Rev. Mod. Phys. **80**, 885 (2008).
[9] X. Chen, Y.-M. Lu, and A. Vishwanath, Nat. Commun. **5**, 3507 (2014).
[10] C. Xu and T. Senthil, Phys. Rev. B **87**, 174412 (2013).
[11] T. Senthil and M. Levin, Phys. Rev. Lett. **110**, 046801 (2013).

[12] S. D. Geraedts and O. I. Motrunich, Ann. Phys. (N.Y.) **334**, 288 (2013).
[13] Z.-X. Liu, Z.-C. Gu, and X.-G. Wen, Phys. Rev. Lett. **113**, 267206 (2014).
[14] N. Regnault and T. Senthil, Phys. Rev. B **88**, 161106 (2013).
[15] S. Furukawa and M. Ueda, Phys. Rev. Lett. **111**, 090401 (2013).
[16] Y.-C. He, S. Bhattacharjee, R. Moessner, and F. Pollmann, Phys. Rev. Lett. **115**, 116803 (2015).
[17] A. Sterdyniak, N. R. Cooper, and N. Regnault, Phys. Rev. Lett. **115**, 116802 (2015).
[18] Y.-H. Wu and J. K. Jain, Phys. Rev. B **87**, 245123 (2013).
[19] J. Dalibard, F. Gerbier, G. Juzeliūnas, and P. Öhberg, Rev. Mod. Phys. **83**, 1523 (2011).
[20] M. Levin and Z.-C. Gu, Phys. Rev. B **86**, 115109 (2012).
[21] M. E. Peskin, Ann. Phys. (N.Y.) **113**, 122 (1978).
[22] C. Dasgupta and B. I. Halperin, Phys. Rev. Lett. **47**, 1556 (1981).
[23] M. P. A. Fisher and D. H. Lee, Phys. Rev. B **39**, 2756 (1989).
[24] A. M. Polyakov, *Gauge Fields and Strings* (Harwood Academic Publishers, Chur, 1987), Vol. 140.
[25] A. Vallat and H. Beck, Phys. Rev. B **50**, 4015 (1994).
[26] M. Cheng and Z.-C. Gu, Phys. Rev. Lett. **112**, 141602 (2014).
[27] X.-G. Wen, Phys. Rev. B **89**, 035147 (2014).
[28] D. H. Lee and G. Grinstein, Phys. Rev. Lett. **55**, 541 (1985).
[29] M. P. A. Fisher, P. B. Weichman, G. Grinstein, and D. S. Fisher, Phys. Rev. B **40**, 546 (1989).
[30] M. Wallin, E. S. Sørensen, S. M. Girvin, and A. P. Young, Phys. Rev. B **49**, 12115 (1994).
[31] L. Bonnes and S. Wessel, Phys. Rev. Lett. **106**, 185302 (2011).
[32] N. Prokof'ev and B. Svistunov, Phys. Rev. Lett. **87**, 160601 (2001).
[33] F. Alet and E. S. Sørensen, Phys. Rev. E **67**, 015701 (2003).
[34] M. Hasenbusch, Int. J. Mod. Phys. C **12**, 911 (2001).
[35] Ş. G. Söyler, B. Capogrosso-Sansone, N. V. Prokof'ev, and B. V. Svistunov, New J. Phys. **11**, 073036 (2009).
[36] R. A. Williams, S. Al-Assam, and C. J. Foot, Phys. Rev. Lett. **104**, 050404 (2010).
[37] J. F. Sherson, C. Weitenberg, M. Endres, M. Cheneau, I. Bloch, and S. Kuhr, Nature (London) **467**, 68 (2010).
[38] R. Pordes *et al.*, J. Phys. Conf. Ser. **78**, 012057 (2007).
[39] I. Sfiligoi, D. C. Bradley, B. Holzman, P. Mhashilkar, S. Padhi, and F. Wurthwein, *2009 WRI World Congress on Computer Science and Information Engineering, Los Angeles, CA* (IEEE, Piscataway, NJ, 2009), Vol. 2, pp. 428–432.
[40] M. Mulligan and M. P. A. Fisher, Phys. Rev. B **89**, 205315 (2014).
[41] U. Wolff, Nucl. Phys. B **810**, 491 (2009).